This article is published as part of a themed issue of ***Photochemical & Photobiological Sciences*** in honour of

Jan Verhoeven

Guest edited by **Anthony Harriman**

Published in **issue 7, 2010**

Communication

Papers

Ultrafast excited-state dynamics of a series of zwitterionic pyridinium phenoxides with increasing sterical hindering†

Guillaume Duvanel,[a] Jakob Grilj,[a] Hélène Chaumeil,[b] Patrice Jacques[c] and Eric Vauthey*[a]

Received 3rd March 2010, Accepted 30th March 2010
First published as an Advance Article on the web 19th April 2010
DOI: 10.1039/c0pp00042f

A series of pyridinium phenoxides that differ by the dihedral angle between the pyridinium and the phenoxide rings because of substituents with increasing steric encumbrance has been investigated by ultrafast spectroscopy. Like the related betaine-30, these molecules are characterised by a zwitterionic electronic ground state and a weakly polar S_1 state. Their fluorescence lifetime was found to lie between 200 to 750 fs, decreasing with increasing dihedral angle, and increasing with solvent viscosity. This was assigned to a non-radiative deactivation of the emissive state coupled to a large amplitude motion involving the dihedral angle. The transient absorption spectra suggested that emission occurs from the Franck–Condon S_1 state, which decays to a dark excited state, that itself most probably corresponds to the relaxed S_1 state. Finally, this relaxed state decays to the vibrationally hot ground state through an intramolecular charge separation process with a time constant ranging between 0.4 and 3 ps, increasing with the dihedral angle and with the solvent relaxation time. These variations were discussed in terms of the Jortner–Bixon model of electron transfer, where the charge separation dynamics depends on both electronic coupling and solvent relaxation. The results suggested that charge separation slows down with increasing dihedral angle.

Introduction

Pyridinium phenoxides or phenolates (PPs) have been shown to be a class of push-pull compounds with promising properties as nonlinear optical materials.[1–4] PPs are zwitterions and are thus characterised by a large permanent electric dipole moment in the electronic ground state, allowing their orientation by poling in an external electric field. Furthermore, the first electronic transition ($S_1 \leftarrow S_0$) is associated with a large change of dipole moment, as testified by the strong negative solvatochromism of the absorption band of most phenolate betaine dyes.[5] In this respect, betaine-30 is one of the most sensitive solvatochromic probes and the energy of its first electronic transition is now widely used as an empirical polarity scale.[6] These PPs are also very attractive molecules for investigating the dynamics of intramolecular charge transfer, as the $S_1 \leftarrow S_0$ transition is associated with a partial charge recombination (CR) process, whereas the non-radiative $S_1 \rightarrow S_0$ transition can be viewed as a partial charge separation (CS). In this case again, betaine-30 is certainly the most investigated PP.[7–16] Barbara and coworkers have performed intensive single-colour transient absorption measurements of the ground-state recovery dynamics of this molecule in various solvents.[7,9,10] The so-obtained rate constants were discussed in terms of the two dimensional Sumi–Marcus model for non-equilibrium electron transfer (ET) modified to take into account nuclear tunnelling as required for a proper description of highly exergonic ET processes. Some of the theoretical parameters, such as the solvent and the intramolecular reorganisation energies, were also determined from the analysis of the absorption band shape. This approach was based on the assumption that the excited-state dynamics of betaine-30 can be discussed in terms of a three level system, *i.e.* that CS back to the zwitterionic hot ground-state occurs directly from the optically-populated excited state. Although good agreement between experiment and theory was obtained, these measurements did not reveal the full details of the excited-state dynamics of betaine-30. A significantly more complex picture has been subsequently revealed by a transient absorption investigation of betaine-30 using broadband detection.[12] It appeared that the excited-state dynamics of this molecule is better accounted for in terms of a four-level system. Indeed, the initially populated excited state undergoes substantial structural rearrangements to end up in a state characterised by a different conformation and smaller electric dipole moment, from which the vibrationally hot zwitterionic ground state is finally repopulated. The initial partial CR process was found to be essentially limited by solvation dynamics, whereas time constants of a few picoseconds were measured for the final CS back to the zwitterionic hot ground state.

Apart from betaine-30, the photophysics of most PPs is poorly documented. We report here on our study of the excited-state dynamics of a series of sterically-hindered PPs (Fig. 1)[4,17] using a combination of femtosecond fluorescence up-conversion and transient absorption spectroscopies. In these PPs, the phenoxyde

[a]*Department of Physical Chemistry, University of Geneva, CH-1211, Geneva 4, Switzerland. E-mail: eric.vauthey@unige.ch*
[b]*Laboratoire de Chimie Organique Bioorganique et Macromoléculaire CNRS FRE 3253, Ecole Nationale Supérieure de Chimie de Mulhouse, Université de Haute Alsace, 3 rue Alfred Werner, 68093, Mulhouse Cedex, France*
[c]*Département de Photochimie Générale, CNRS FRE 3252, Ecole nationale Supérieure de Chimie de Mulhouse, Université de Haute Alsace, 3 rue Alfred Werner, 68093, Mulhouse Cedex, France*

† This article is published as part of a themed issue in appreciation of the many important contributions made to the field of molecular photophysics by Jan Verhoeven.

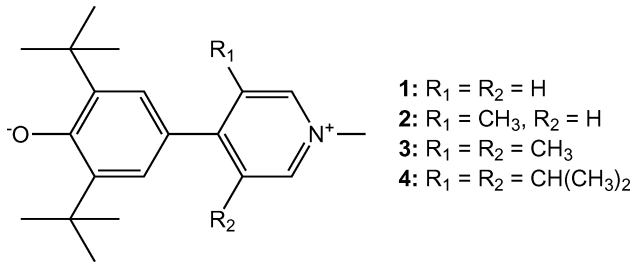

Fig. 1 Pyridinium phenoxides (PPs) **1–4**.

group is attached to the carbon atom in the *para* position relative to the pyridinium nitrogen, and not directly to the nitrogen atom as it is the case for betaine-30. The *tert*-butyl groups in the *ortho* position of the phenoxide function limit protonation, most probably through steric hinderance, and favour solubility, hence reducing aggregation. On the other hand, alkyl groups of varying size in the *meta* position of the pyridinium group allow for a control of the dihedral angle between the pyridinium and phenoxide rings. According to semi-empirical quantum chemistry calculations, this dihedral angle varies from about 10° in **1** to ~50° in **4**.[4] This coordinate has been suggested to play a significant role in the ET dynamics of betaine-30,[12,16,18] as well as in the nonlinear optical properties of zwitterions.[4,19] The quadratic optical properties of this series of PPs have recently been reported,[4] and increasing nonlinear response with increasing torsion angle was indeed found. The aim of the present study is first to explore the influence of the dihedral angle on their intramolecular ET dynamics and second to see how the excited-state dynamics of these PPs differs from that of betaine-30.

Experimental

The synthesis of **1–4** has been described in detail in ref. 17. The solvents, acetonitrile (ACN, puriss. p.a., Sigma), chloroform ($CHCl_3$, puriss. p.a., Sigma), ethanol (EtOH, puriss. p.a. Fluka) and 1-butanol (BuOH, puriss. p.a. Merck) were used as received.

Steady-state measurements

Absorption spectra were recorded on a Cary 50 spectrophotometer, whereas stationary fluorescence was tentatively measured on a Cary Eclipse fluorimeter.

Fluorescence up-conversion (FU)

The FU setup was the same as described previously,[20] except that excitation was performed at 500 nm using the frequency doubled output of a Kerr lens mode-locked Ti:Sapphire laser (Mai Tai, Spectra-Physics). The polarization of the pump pulses was at magic angle relative to that of the gate pulses at 1000 nm. The pump intensity on the sample was on the order of 5 μJ cm^{-2} and the fullwidth at half-maximum (fwhm) of the instrument response function was *ca.* 210 fs. The sample solutions were located in a 0.4 mm rotating cell and had an absorbance of about 0.1 at 500 nm.

Transient absorption (TA)

The experimental setup has been described in detail earlier.[21,22] Excitation was carried out at 530 nm with a home-built two-stage non-collinear optical parametric amplifier. The pump intensity on the sample was *ca.* 1–2 mJ cm^{-2}. The polarization of the probe pulses was at magic angle relative to that of the pump pulses. All spectra were corrected for the chirp of the white-light probe pulses. The fwhm of the response function was *ca.* 150 fs. The sample solutions were placed in a 1 mm thick quartz cell and were continuously stirred by N_2 bubbling. Their absorbance at the excitation wavelength was around 0.3. No significant degradation of the samples was observed except with **1** in EtOH, for which a ~20% decrease of the absorption band was observed after measurements.

Results

Steady-state spectra

The VIS absorption spectra of **1–4** in ACN are shown in Fig. 2. These spectra consist in a broad absorption band, typical of a charge transfer transition, with a maximum wavelength that increases by going from **1** to **4**, *i.e.* upon increasing dihedral angle. The band of **1** presents some structure, indicative of a possible smaller charge transfer character of the transition. As expected for zwitterionic betaines, this absorption band exhibits a strong negative solvatochromism. The latter is about the same for **1** and **2** but increases with **3** and **4**. The solvent dependence of these compounds will be discussed in detail below. However, their strong hypsochromic shift confirms the CR nature of its associated transition.

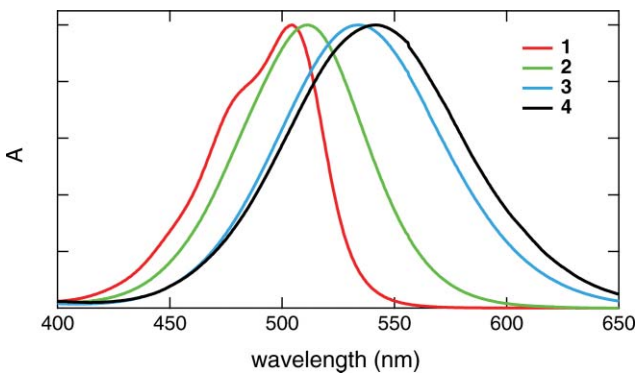

Fig. 2 Visible absorption spectra of **1–4** in ACN.

No stationary emission could be observed with any of **1–4**, indicative of a fluorescence quantum yield inferior to ~10^{-4}, and thus pointing to a very short excited-state lifetime.

Time-resolved fluorescence

Despite the lack of stationary emission, a fluorescence up-conversion signal could be observed at wavelengths located above the maximum of the $S_1 \leftarrow S_0$ absorption band. Fig. 3A shows time profiles of the fluorescence intensity at different wavelengths recorded with **1** in EtOH. A slowing down of the fluorescence dynamics with increasing wavelength can clearly be observed. These time profiles could be analyzed globally using the convolution of the instrument response function with a biexponential function using the same pair of time constants, $\tau_{f1} = 0.15$ ps and $\tau_{f2} = 0.39$ ps, and the amplitudes shown in Fig. 3B. As

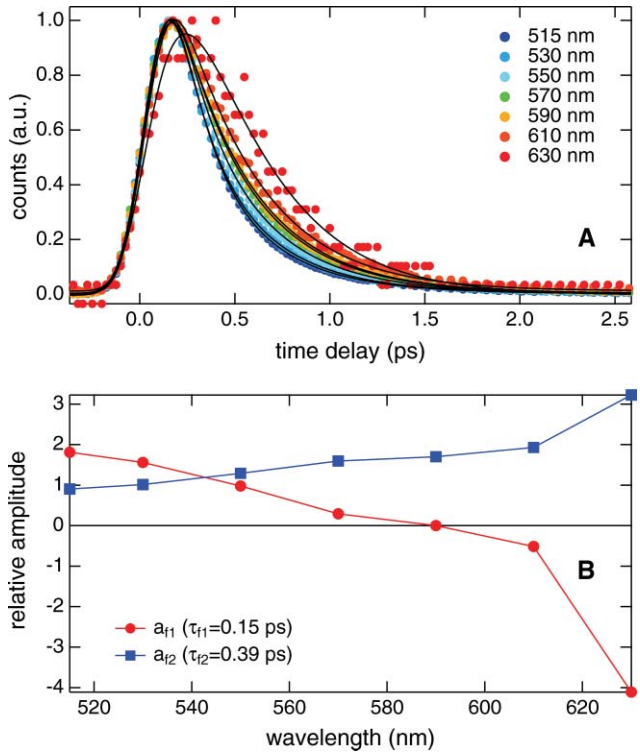

Fig. 3 (A) Intensity-normalised fluorescence time profiles of **1** in EtOH recorded at various wavelengths upon 500 nm excitation. (B) Wavelength dependence of the amplitudes obtained upon global analysis of the fluorescence dynamics of **1** in EtOH.

no stationary fluorescence spectrum could be measured, decay associated emission spectra could not be reconstructed and the amplitudes displayed in Fig. 3B are those directly obtained from the analysis of the intensity-normalised time profiles. Whereas a_{f2}, the amplitude related to the longest time constant, is positive at all wavelengths measured, that related to τ_{f1} is positive below 590 nm and negative above. Therefore, the latter time constant is associated with a red shift of the fluorescence spectrum. According to the value of τ_{f1}, this effect is most probably due to the solvation of the excited state, *i.e.* to a dynamic Stokes shift. Solvent relaxation in EtOH has been reported to occur on various timescales with sub-picosecond time constants associated with inertial motion and time constants of 5 and 30 ps due to diffusive motion.[23] On the other hand, as a_{f2} is positive at all wavelengths, the time constant $\tau_{f2} = 0.39$ ps can be interpreted as the decay time of the emitting population. As this population is extremely short-lived, only the fastest component of the solvation dynamics can be observed in the dynamic Stokes shift. In addition to the solvent, relaxation of intramolecular modes could also contribute to this shift.

The time profiles of the fluorescence measured with the other PPs in EtOH are very similar and have thus been analyzed in the same way. The resulting time constants are listed in Table 1. The amplitudes, a_{f1} and a_{f2} of the biexponential function exhibit a similar wavelength dependence than with **1** and thus the time constants, τ_{f1} and τ_{f2} can be interpreted alike. A shortening of both time constants can be observed by going from **1** to **4**. As τ_{f1} is noticeably shorter than the instrument response function of the FU setup, these differences should be considered with caution. On the other hand, the decrease of τ_{f2} by going from **1** to **2** and from

Table 1 Time constants obtained from the global analysis of the fluorescence up-conversion profiles measured at different wavelengths with various PP/solvent systems, and solvent properties (error on τ_f: ±10%)

PP	Solvent	ε_s[a]	$E_T(30)$/ kcal mol^{-1}	η[b]/cP	τ_{f1}/ps	τ_{f2}/ps
1	ACN	37.5	45.6	0.34	0.12	0.25
1	$CHCl_3$	4.8	39.1	0.54	0.16	0.37
1	EtOH	24.5	51.9	1.08	0.15	0.39
1	BuOH	17.5	49.7	2.6	0.22	0.75
1	EtOH				0.15	0.39
2	EtOH				0.10	0.25
3	EtOH				0.08	0.18
4	EtOH				0.07	0.20

[a] Dielectric constant. [b] Viscosity.

2 to **3** and **4** is more significant. Consequently, these results point to a fluorescence lifetime that decreases with increasing dihedral angle between the pyridinium and phenoxide rings.

The fluorescence dynamics of **1** has also been investigated in three other solvents, namely $CHCl_3$, BuOH and ACN. In these cases again, the time profiles could be well reproduced using a biexponential function with the time constants listed in Table 1. It appears that τ_{f1} does not exhibit a strong solvent dependence, in agreement with its assignment to inertial solvent motion. As excitation is performed slightly on the blue side of the absorption band, some vibrational relaxation could also contribute to this dynamic component.

On the other hand, τ_{f2} manifests a more marked solvent dependence and increases by a factor of 3 by going from ACN to BuOH. Table 1 indicates that there is no simple correlation between τ_{f2} and a single solvent property, but an increase of τ_{f2} with the solvent viscosity can be discerned. However, considering that τ_{f2} is the same in EtOH and $CHCl_3$, and that EtOH is twice as viscous as $CHCl_3$, it appears that other solvent properties like solvent polarity, expressed either in terms of the dielectric constant or the empirical $E_T(30)$ scale, must also influence this time constant. Such combined influence of solvent polarity and viscosity has already been reported for the photoisomerization of cyanines and for other processes involving structural changes of polar molecules.[24–26]

Transient absorption

The TA spectra recorded with **1** in EtOH at various time delays after 530 nm excitation are depicted in Fig. 4. At short time delay (Fig. 4A), the spectra are dominated by a negative TA band that corresponds to the bleach of the $S_1 \leftarrow S_0$ absorption band. Additionally, a weaker negative feature extending from 550 to more than 700 nm can be observed. After about 300 fs, this feature is no longer visible and is replaced by a small positive TA band at ~560 nm. According to its position and lifetime, this negative band can be rather safely ascribed to stimulated emission. The 560 nm band is ascribed to the absorption of a dark, non-emissive, intermediate. The TA spectra recorded on a longer timescale (Fig. 4B) show a substantial decrease of the bleach accompanied by the growth and the blue shift of the positive band. This band reaches its maximum intensity after about 3.5 ps. From then on, its position remains unchanged and its intensity decays to zero within a few tens of picoseconds, in parallel with the decay of the bleach. The same measurements have been repeated in ACN,

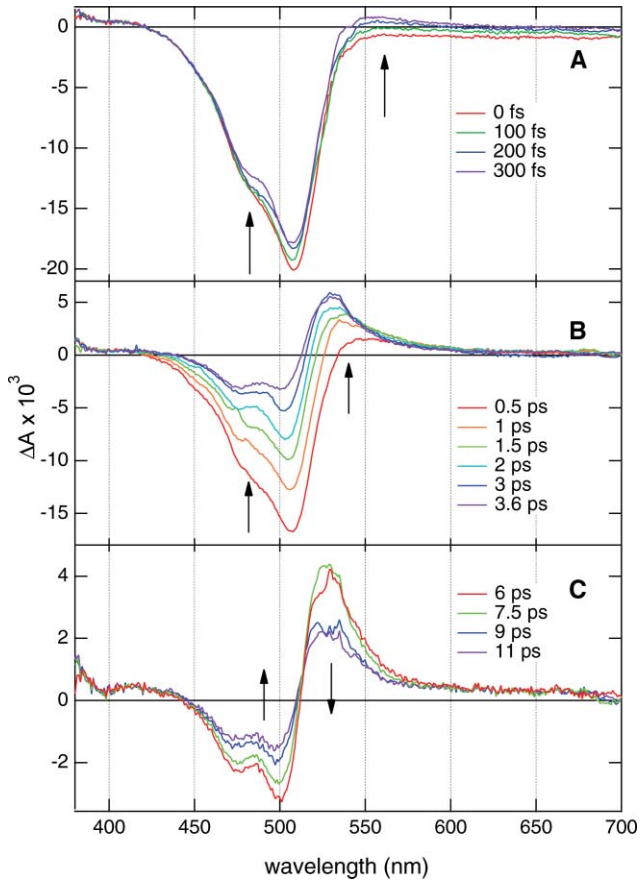

Fig. 4 Transient absorption spectra recorded with **1** in EtOH at different time delays after 530 nm excitation.

$CHCl_3$ and BuOH and yielded very similar TA spectra. TA spectra of **2** were also recorded in all four solvents, whereas **4** was only investigated in ACN. In these cases again, no significant differences with the spectra shown in Fig. 4 were observed, with the exception of the position of the negative band stemming from the bleach of the $S_1 \leftarrow S_0$ absorption and the timescale associated with the spectral changes.

The spectra measured at various time delays with a given PP/solvent system have been analyzed globally using a sum of exponential functions. A good fit was obtained with three to four exponential functions, with the time constants listed in Table 2. The decay-associated spectra resulting from such an analysis with **1** in EtOH are illustrated in Fig. 5, those obtained with the other systems being qualitatively very similar. This figure reveals that the spectrum associated with the shortest time constant ($\tau_1 = 0.45$ ps) is negative above 550 nm, where stimulated emission dominates the TA spectra at very early time. Thus, this time constant can be safely ascribed to the decay of the stimulated emission and to the decay of the Franck–Condon (FC) excited state population. This interpretation is supported by the resemblance of this time constant, τ_1, with τ_{f2} obtained from the FU measurements. The positive feature around 500 nm could be due either to the absorption of this emitting state or to some artefact originating from the data analysis, as the shape of this band resembles that of the bleach of the ground state absorption and as the time constant is close to the instrument response function.

Table 2 Time constants obtained from the global analysis of the transient absorption spectra measured with various PP/solvent systems and tentative assignment according to the decay-associated spectra (**bold**: decay of the FC state population; *italic*: decay of the dark state population; underlined: vibrational cooling; normal: ambiguous, probably mixed contributions. Error on τ: ±15%, unless marked with a '~')

PP	Solvent	τ_1/ps	τ_2/ps	τ_3/ps	τ_4/ps
1	ACN	**0.3**	*0.4*	1.2	11
1	$CHCl_3$	**0.5**	*0.8*	1.9	14
1	EtOH	**0.45**	*1.2*	5.0	~50
1	BuOH	**0.9**	1.6	*3.0*	15
2	ACN	**0.35**	*0.9*	9.2	
2	$CHCl_3$	**0.6**	0.9	*2.2*	15
2	EtOH	**0.45**	*3.3*	7.8	~60
2	BuOH	**1.0**	2.6	*7.7*	~90
4	ACN	**0.5**	*1.5*	12	

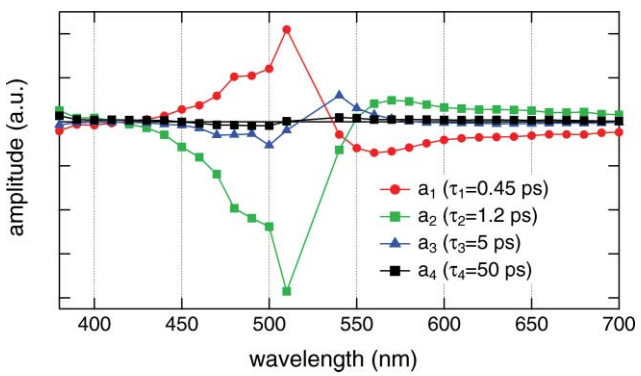

Fig. 5 Decay-associated spectra obtained from global multiexponential analysis of the TA spectra measured with **1** in EtOH.

The spectrum associated with τ_2 is characterised by an intense negative band at 500 nm, pointing to a substantial recovery of the ground-state population. The positive band above 550 nm suggests that the decay of the dark excited state takes place with this time constant as well. Finally, the spectra related to the two largest time constants, τ_3 and τ_4, show a negative band in the $S_1 \leftarrow S_0$ absorption region and a positive band at its red edge. Such spectra are typical of hot ground-state absorption.[27,28] Indeed, the optical transition from the vibrationally hot ground state is shifted to longer wavelengths compared to that occurring from the lowest vibrational state. Consequently, the transient absorption spectrum is characterised by a negative band arising from the depletion of the vibrationally relaxed ground-state population, together with a nearby, partially overlapping, positive band due to the population of the vibrationally hot ground state. The positive band in the τ_4 spectrum is slightly blue shifted relative to that in the τ_3 spectrum. This effect can be explained by the fact that the absorption spectrum of the hot ground state progressively shifts to shorter wavelengths as vibrational cooling takes place.

A similar analysis has been performed with the other PP/solvent systems and the resulting time constants together with their

assignment are listed in Table 2. In some cases, the assignment of τ_2 was ambiguous as the associated spectrum indicated both stimulated emission and dark state decay. Most probably, the dynamics of these processes is not purely mono-exponential and thus several processes could show up in a given time constant. A non-exponential dynamics would not be surprising here, considering that population decay occurs on a similar timescale as those of solvent and vibrational relaxation. Such non-exponential population dynamics has, for example, been observed with the CR of excited donor–acceptor complexes in polar solvents.[29,30]

By comparing these time constants with those obtained from the FU measurements (Table 1), a good agreement between τ_1 and τ_{f2} can generally be observed, with some exceptions such as **2** in EtOH. However, considering the strong overlap of the bands associated with stimulated emission, with dark excited state and hot ground state absorption, it appears that τ_1 could partially originate from other contributions than from the decay of the stimulated emission only. Therefore, the time constant obtained from FU, τ_{f2}, most certainly better describes the decay of the emissive FC state population than that obtained from the analysis of the TA spectra.

Discussion

From the above results, it appears that the excited-state dynamics of all four PPs investigated here can be well accounted for by a four level scheme:

$$S_0 \xrightarrow{h\nu} S_1^{FC} \xrightarrow{\text{relaxation}} S_1^{rel} \xrightarrow{CS} S_0^{hot} \xrightarrow{VC} S_0 \qquad (1)$$

where VC stands for vibrational cooling. A similar scheme has already been proposed earlier to explain the dynamics observed with betaine-30 in polar solvents.[12] Considering the similar structures of **1–4** and betaine-30, such resemblance is not surprising. Global analysis of the TA spectra with target analysis based of this scheme has also been tried. It should be noted that the time constants found assuming four successive first order processes are in principle the same as those obtained from a global analysis with the sum of four exponential functions, and that the resulting species-associated spectra are linear combinations of the decay associated spectra.[31] However, considering that the different steps of the excited-state dynamics of the PPs are ultrafast and do not follow purely monoexponential dynamics, the species-associated spectra obtained assuming a simple succession of four processes following a first order kinetics most certainly do not reflect the actual spectra of the various intermediates. This probably explains why the so-obtained 'species' spectra were very similar to the decay associated spectra. Consequently, these spectra were not further considered.

The transition from the FC excited state to the dark excited state most likely involves structural and solvent relaxation as in betaine-30. In fact, the dark excited state most probably corresponds to the thermally equilibrated S_1 state. Because of substantial structural differences, the S_0 and the S_1 potentials should be strongly displaced and thus the minimum of the S_1 potential cannot be directly reached optically from S_0, as also seen through the decreasing oscillator strength when comparing molecules with increasing dihedral angle. For the same reason, emission from the relaxed S_1 state has essentially no dipolar strength. Structural and solvent relaxation can also be expected to lead to a further decrease of the electric dipole moment of the PPs. Thus, the time constants obtained from the FU measurements reflect this excited-state relaxation, with τ_{f1} being essentially due to the inertial part of solvation and to the relaxation of high frequency intramolecular modes, and with τ_{f2} corresponding mainly to the relaxation of lower frequency modes. After this process, the relaxed excited state is no longer fluorescent and thus the slower stage of solvent relaxation cannot be observed in the fluorescence dynamics.

As mentioned above, τ_{f2} seems to be correlated with solvent viscosity (Table 1). This suggests that the structural relaxation involves some large amplitude motion, most probably a twist around the single bond between the pyridinium and the phenoxide rings.

Interestingly, τ_{f2} measured in a single solvent, EtOH, decreases when going from **1** to **4**, namely with increasing dihedral angle of the PP. This correlation agrees with the hypothesis of a twisted relaxed excited state. Indeed, if the PP is already twisted in the ground state because of the presence of the substituents on the pyridinium ring, the FC excited state is itself already pre-twisted and thus relaxation should involve smaller structural changes and can thus be expected to be faster, as found here. However, it should be kept in mind that the zwitterionic form is only one of the limit structures of the PPs, the other being the quinone form. The zwitterionic structure can be expected to be favored by an increasing torsion angle. This idea is supported by the slightly structured absorption band of **1** (Fig. 2) that could be due to a larger quinone character. As a consequence, the excited-state relaxation of the less twisted PPs could not only involve a larger torsional motion but also require different rearrangements of other intramolecular modes.

The large electron density at the phenoxide oxygen in the ground-state should strongly favor H-bonding in both EtOH and BuOH. At the same time, the H-bond strength should be strongly reduced in the excited state because of its much weaker polarity. Thus, H-bonds to the solvent should not play a significant role in the deactivation of the S_1 state of **1–4** in protic solvents. If this was the case, τ_{f2} would be shorter in EtOH and BuOH than in non-protic solvents, as found for H-bond-assisted non-radiative deactivation.[32–35] Furthermore, if excited-state proton transfer was taking place, the protonated form of the PPs would have been observed. Protonated **1–4** PPs start to absorb just below 400 nm and fluoresce in the visible region.[36] If these species were formed, they would have been observed either by TA as the spectral window of the setup extends down to 350 nm, or by fluorescence. In any case, both H-bond-assisted non-radiative deactivation and intermolecular excited-state proton transfer occurs in the 10^{-10}–10^{-8} s timescale,[32–35] and are thus too slow to take place within the ultrashort excited-state lifetime of the PPs.

As the excited state is much less polar than the ground state, its decay back to S_0 can be considered as an intramolecular CS. The time constants ascribed to this process, τ_{CS}, are listed in italic in Table 2. The latter shows that, for both **1** and **2**, τ_{CS} increases in the order ACN < $CHCl_3$ < EtOH < BuOH. This sequence does not correlate with the dielectric constant or the $E_T(30)$ polarity scale but follows the same trend as viscosity and solvation dynamics. However, the latter is known to be strongly multiphasic,[37,38] and τ_{CS} in **1** would rather correspond to the faster components of solvation. On the other hand, if we compare τ_{CS} in a single solvent,

like for example ACN, we can see an increase in the order **1**, **2** and **4**, *i.e.* with increasing dihedral angle. The same trend can be also observed in the other solvents with **1** and **2**. In fact CS in **2** is about 2.5 times as slow as in **1**, independent of the solvent. This increase of τ_{CS} with increasing twist angle could be explained by a reduction of the electronic coupling V for ET. Indeed, the CS dynamics in these PPs can be qualitatively rationalized using the Jortner–Bixon model, with the ET rate constant given by:[39]

$$k_{ET} = \frac{k_{NA}}{1+\kappa} \tag{2}$$

where k_{NA} is the rate constant for a non-adiabatic ET, which, in its semiclassical form, can be expressed as:[40,41]

$$k_{NA} = \frac{2\pi}{\hbar} V^2 (4\pi\lambda_1 k_B T)^{-1/2} \sum_{n=0}^{\infty} \frac{S^n}{n!} \exp(-S) \exp\left[-\frac{(\Delta G_{ET} + n\hbar\omega + \lambda_1)^2}{4\lambda_1 k_B T} \right] \tag{3}$$

where λ_1 is the reorganization energy of the low frequency modes, S the Huang–Rhys factor, ω the average frequency of the vibrational modes coupled to ET with the vibrational quantum number n and ΔG_{ET} the driving force.

In eqn(2), κ is a so-called adiabaticity parameter:

$$\kappa = \frac{4\pi V^2 \tau_L}{\hbar \lambda_1} \tag{4}$$

where τ_L is the longitudinal dielectric relaxation time of the solvent.

Eqn(2) reveals that, if the adiabaticity parameter is sufficiently large, the ET rate constant depends on both the electronic coupling and the solvent dynamics. The electronic coupling V for CS in **1–4** back to the ground-state is not known. In principle, V can be estimated from the oscillator strength of the charge transfer optical transition, f:[42]

$$f = \frac{8\pi^4 m_e}{3h^3 e^2 \nu_{av}} (V\Delta\mu)^2 \tag{5}$$

where m_e is the mass and e the charge of the electron, h the Planck constant, ν_{av} the average frequency and $\Delta\mu$ the dipole moment difference between the ground and excited states. The determination of V requires knowledge of the oscillator strength for the optical transition from the relaxed excited state. As this quantity is not accessible, we can use, as an upper limit, the oscillator strength for the transition from the ground state to the FC excited state, which has been shown to decrease from 0.65 to 0.25 by going from **1** to **4**.[4] The dipole moment difference $\Delta\mu$ is not known either. However, the permanent electric dipole moment of the ground state of **1–4** has been calculated to range between 21 and 25 D.[4] With a value of 20 D for $\Delta\mu$, eqn(5) yields an electronic coupling $V = 0.3$ eV for **1**, which decreases continuously down to $V = 0.2$ eV for **4**. Once again, these are upper-limit values, as the lack of emission from the relaxed excited state points to a much smaller oscillator strength of the transition to the ground state. Thus a 100 times smaller f value, corresponding to V of the order of 0.02–0.03 eV (~200 cm^{-1}), and an average τ_L of 0.26 ps for ACN, the fastest solvent, and of 63 ps for BuOH, the slowest one,[23] give adiabaticity parameters, κ, in the range of 1.8 for **4** in ACN up to 1.2×10^4 for **1** in BuOH. These estimates for κ reveal that CS back to the ground state is not purely non-adiabatic and thus its rate constant depends on both V and solvation time.

The increase of τ_{CS} from **1** to **4** in a given solvent can be explained by a decrease of V, which could originate from different twist angles of the relaxed S_1 state. However, the shortening of the fluorescence lifetime τ_{f2} observed by going from **1** to **4** suggested that the extent of structural change decreases accordingly and that the twist angle of the four PPs should differ less than in the ground state. However, as the reduction of V with increasing dihedral angle should follow a cosine dependence, a variation of the angle around 80–90° will have a much stronger effect on V than a change around 10–50°, the ground-state values.

However, one should also keep in mind that the presence of substituents with increasing bulkiness on the pyridinium ring implies larger delocalization of the electric charges and thus a smaller electronic coupling.[43] Consequently, the variation of τ_{CS} cannot be unambiguously ascribed to a different dihedral angle of the relaxed excited state. Moreover, other factors such as the driving force could also contribute to the observed difference in CS dynamics. Indeed, the redox properties of aromatic compounds can be easily tuned by varying the size of alkyl substituents.[44] This effect is probably at the origin of the red shift of the $S_1 \leftarrow S_0$ absorption band observed by going from **1** to **4**.

On the other hand, the solvent dependence of τ_{CS} can be accounted for by an increase of κ by going from ACN to BuOH. However, according to eqn(2) and (4), a κ of 1.2×10^4, as calculated for **1** in BuOH, would imply that $\tau_{CS} \propto \tau_L$. This is clearly not the case here as CS in BuOH is much faster that the average solvation time of 63 ps. ET faster than solvation has been described theoretically by Sumi and Marcus using a two dimensional description of the reaction coordinate.[45,46] Whereas in conventional ET theories the solvent is in permanent quasi-equilibrium with the system during the reaction,[41] in the Sumi–Marcus model, ET can occur before all the solvent modes have fully relaxed. Such ET faster than solvation is possible when the process is sufficiently exergonic to be operative even in weakly or non-polar environments. This is of course the case here as CS occurs from an excited state down to the ground state. Such non-equilibrium ET dynamics has also been invoked to account for the excited-state dynamics of betaine-30.[7,10]

Finally, Table 2 shows that, in most cases, two exponential functions are needed to account for the relaxation of the vibrationally hot ground state. Such multiphasic behavior has already been reported for vibrational cooling.[28,47,48] However, in most cases the largest time constant was rather on the order of 10 ps, *i.e.* smaller than that found for **1** in EtOH and for **2** in EtOH and BuOH. In the case of **1** in EtOH, this longer time constant may also partially arise from a slight photo-degradation of the sample. Moreover, given that in those three cases, the amplitude associated with τ_4 was very small, the error on this time constant is large. On the other hand, the early steps of vibrational cooling that occur on similar or even faster timescale than CS are missed here. The solvent dependence of vibrational energy relaxation is still not totally understood.[28,47–51] Some groups have observed a strong correlation between the vibrational cooling dynamics and the thermal diffusivity of the solvent.[52,53] Such a relationship cannot be found here. For example, ACN and EtOH have a similar thermal diffusivity ($D_{th} \sim 10^{-7}$ m^2 s^{-1})[47,54] but the measured

vibrational cooling dynamics is very different in these two solvents. On the other hand, other investigations point to an acceleration of vibrational cooling by the presence of H-bonds between the solute and the solvent molecules.[28,47] From Table 2, vibrational cooling seems rather to be the slowest in the H-bonding solvents. However, the occurrence of cooling components faster than CS cannot be excluded. This would also explain the very low amplitude associated with τ_4 in protic solvents. Therefore, as only relaxation components slower then CS can be observed here, no definitive conclusion on the solvent dependence of VR can be drawn from the present results.

Conclusions

The excited-state dynamics of the pyridinium phenoxides investigated here exhibit many similarities with that of betaine-30. First, it is best accounted for in terms of a four level scheme, as suggested by Kovalenko *et al.* for betaine-30. Indeed, the FC excited state, that exhibits fluorescence, rapidly relaxes to a dark state that itself decays to the zwitterionic ground state through a partial intramolecular CS process. If we compare the characteristic time constants for the decay of the FC excited state and for the ensuing CS in betaine-30, it appears that both processes are very similar to those measured here with **4**, *i.e.* with the most twisted PP. This resemblance is not really surprising as betaine-30 is known to be twisted in the ground state because of the steric hindrance introduced by the phenyl substituents. Quantum chemistry calculations of betaine-30 predict a dihedral angle of 52°, *i.e.* very close to that calculated for **4**.[18] The CS in other PPs are substantially faster than in betaine-30. We have suggested here that these differences in CS dynamics are due to the twist angle that controls the electronic coupling. However, this effect could also be due, at least partially, to the different substituents on the pyridinium ring used to introduce the steric constraint. In this case, the resembling CS dynamics of betaine-30 and **4** could simply originate from a similar effect of both phenyl and isopropyl groups on the electronic coupling and/or on the driving force. Unfortunately, these two effects cannot be easily separated. Despite this, the results presented here should contribute to a better understanding of the photophysics of this important class of molecules.

Acknowledgements

This work was supported by Swiss National Science Foundation (grant No. 200020-115942).

Notes and references

1 A. Boeglin, A. Fort, L. Mager, C. Combellas, A. Thièbault and V. Rodriguez, Geometrical structure and nonlinear optical response of a zwitterionic push-pull biphenyl compound, *Chem. Phys.*, 2002, **282**, 353–360.
2 R. Zalesny, W. Bartkowiak, S. Styrcz and J. Leszczynski, Solvent Effects on Conformationally Induced Enhancement of the Two-Photon Absorption Cross Section of a Pyridinium-N-Phenolate Betaine Dye. A Quantum Chemical Study, *J. Phys. Chem. A*, 2002, **106**, 4032–4037.
3 W. Niewodniczański and W. Bartkowiak, Theoretical study of geometrical and nonlinear optical properties of pyridinum N-phenolate betaine dyes, *J. Mol. Model.*, 2007, **13**, 793–800.
4 A. Boeglin, A. Barsella, A. Fort, F. Mançois, V. Rodriguez, V. Diemer, H. Chaumeil, A. Defoin, P. Jacques and C. Carré, Optical properties and progressive sterical hindering in pyridinium phenoxides, *Chem. Phys. Lett.*, 2007, **442**, 298–301.
5 C. Runser, A. Fort, M. Barzoukas, C. Combellas, C. Suba, A. Thièbault, R. Graff and J. P. Kintzinger, Solvent effect on the intramolecular charge transfer of zwitterions. Structures and quadratic hyperpolarizabilities, *Chem. Phys.*, 1995, **193**, 309–319.
6 C. Reichardt, Solvatochromic Dyes as Solvent Polarity Indicators, *Chem. Rev.*, 1994, **94**, 2319–2358.
7 G. C. Walker, E. Akesson, A. E. Johnson, N. E. Levinger and P. F. Barbara, Interplay of solvent motion and vibrational excitation in electron transfer kinetics: experiment and theory., *J. Phys. Chem.*, 1992, **96**, 3728.
8 P. F. Barbara, G. C. Walker and T. P. Smith, Vibrational Modes and the Dynamic Solvent Effect in Electron and Proton Transfer, *Science*, 1992, **256**, 975–981.
9 A. E. Johnson, N. E. Levinger, W. Jarzeba, R. E. Schlief, D. A. V. Kliner and P. F. Barbara, Experimental and theoretical study of inhomogeneous electron transfer in betaine: comparison of measured and predicted spectral dynamics., *Chem. Phys.*, 1993, **176**, 555.
10 P. J. Reid and P. F. Barbara, Dynamic solvent effect on Betaine-30 electron transfer kinetics in alcohols, *J. Phys. Chem.*, 1995, **99**, 3554.
11 S. R. Mente and M. Maroncelli, Computer Simulations of the Solvatochromism of Betaine-30, *J. Phys. Chem. B*, 1999, **103**, 7704–7719.
12 S. A. Kovalenko, N. Eilers-König, T. Senyushkina and N. P. Ernsting, Charge Transfer and Solvation of Betaine-30 in Polar Solvents: A Femtosecond Broadband Transient Absorption Study, *J. Phys. Chem. A*, 2001, **105**, 4834.
13 W. Werncke, S. Wachsmann-Hogiu, J. Dreyer, A. I. Vodchits and T. Elsaesser, Ultrafast intramolecular electron transfer studied by picosecond and stationary Raman spectroscopy, *Bull. Chem. Soc. Jpn.*, 2002, **75**, 1049–1055.
14 X. Zhao, J. A. Burt and J. L. McHale, Resonance Raman analysis of nonlinear solvent dynamics: Betaine-30 in ethanol, *J. Chem. Phys.*, 2004, **121**, 11195–11201.
15 T. Ishida and P. J. Rossky, Consequences of Strong Coupling between Solvation and Electronic Structure in the Excited State of a Betaine Dye, *J. Phys. Chem. B*, 2008, **112**, 11353–11360.
16 V. Kharlanov and W. Rettig, Experimental and Theoretical Study of Excited-State Structure and Relaxation Processes of Betaine-30 and of Pyridinium Model Compounds, *J. Phys. Chem. A*, 2009, **113**, 10693–10703.
17 V. Diemer, H. Chaumeil, A. Defoin, A. Fort, A. Boeglin and C. Carré, Syntheses of Sterically Hindered Zwitterionic Pyridinium Phenolates as Model Compounds in Nonlinear Optics, *Eur. J. Org. Chem.*, 2008, 1767–1776.
18 J. Lobaugh and P. J. Rossky, Computer Simulation of the Excited State Dynamics of Betaine-30 in Acetonitrile, *J. Phys. Chem. A*, 1999, **103**, 9432–9447.
19 I. D. L. Albert, T. J. Marks and M. A. Ratner, Remarkable NLO Response and Infrared Absorption in Simple Twisted Molecular pi-Chromophores, *J. Am. Chem. Soc.*, 1998, **120**, 11174–11181.
20 A. Morandeira, E. Vauthey, A. Schuwey and A. Gossauer, Ultrafast excited state dynamics of tri- and hexaporphyrin arrays, *J. Phys. Chem. A*, 2004, **108**, 5741–5751.
21 G. Duvanel, N. Banerji and E. Vauthey, Excited-State Dynamics of Donor–Acceptor Bridged Systems Containing a Boron-Dipyrromethene Chromophore: Interplay between Charge Separation and Reorientational Motion, *J. Phys. Chem. A*, 2007, **111**, 5361–5369.
22 N. Banerji, G. Duvanel, A. Perez-Velasco, S. Maity, N. Sakai, S. Matile and E. Vauthey, Excited-state dynamics of hybrid multichromophoric systems: toward an excitation wavelength control of the charge separation pathways, *J. Phys. Chem. A*, 2009, **113**, 8202–8212.
23 M. L. Horng, J. A. Gardecki, A. Papazyan and M. Maroncelli, Subpicosecond Measurements of polar solvation dynamics: Coumarin 153 Revisited, *J. Phys. Chem.*, 1995, **99**, 17311–17337.
24 M. Van der Auweraer, M. Van den Zegel, N. Boens, F. C. De Schryver and F. Willig, Photophysics of 2-phenyl-3-indolocarbocyanine dyes, *J. Phys. Chem.*, 1986, **90**, 1169–1175.
25 J. Hicks, M. Vandersall, Z. Babarogic and K. B. Eisenthal, The dynamics of barrier crossings in solution: The effect of a solvent polarity-dependent barrier, *Chem. Phys. Lett.*, 1985, **116**, 18.
26 I. Petkova, G. Dobrikov, N. Banerji, G. Duvanel, R. Perez, D. Dimitrov, P. Nikolov and E. Vauthey, Tuning the excited-state dynamics of GFP-inspired imidazolone derivatives, *J. Phys. Chem. A*, 2010, **114**, 10–20.

27 H. Miyasaka, M. Hagihara, T. Okada and N. Mataga, 'Femtosecond laser photolysis studies on the cooling process of chrysene in the vibrationallly hot S1 state in solution, *Chem. Phys. Lett.*, 1992, **188**, 259.
28 S. A. Kovalenko, R. Schanz, H. Hennig and N. P. Ernsting, Cooling dynamics of an optically excited molecular probe in solution from femtosecond broadband transient absorption spectrsocopy, *J. Chem. Phys.*, 2001, **115**, 3256.
29 R. G. Fedunov, S. V. Feskov, A. I. Ivanov, O. Nicolet, S. Pagès and E. Vauthey, Effect of the excitation pulse carrier frequency on the ultrafast charge recombination dynamics of donor–acceptor complexes: Stochastic simulations and experiments, *J. Chem. Phys.*, 2004, **121**, 3643.
30 O. Nicolet, N. Banerji, S. Pagès and E. Vauthey, Effect of the Excitation Wavelength on the Ultrafast Charge Recombination Dynamics of Donor–Acceptor Complexes in Polar Solvents, *J. Phys. Chem. A*, 2005, **109**, 8236.
31 J. E. Loefroth, Time-resolved emission spectra, decay-associated spectra, and species-associated spectra, *J. Phys. Chem.*, 1986, **90**, 1160–1168.
32 S. R. Flom and P. F. Barbara, Proton transfer and hydrogen bonding in the internal conversion of S1 anthraquinones, *J. Phys. Chem.*, 1985, **89**, 4489–4494.
33 T. Nishiya, S. Yamauchi, N. Hirota, M. Baba and I. Hanazaki, Fluorescence study of the intramolecularly hydrogen-bonded molecules o-hydroxyacetophenone and salicylamide and related molecules, *J. Phys. Chem.*, 1986, **90**, 5730–5735.
34 A. Fürstenberg and E. Vauthey, Excited State Dynamics of the Fluorescent Probe Lucifer Yellow in Liquid Solutions in in Heterogeneous Media, *Photochem. Photobiol. Sci.*, 2005, **4**, 260–267.
35 P. S. Sherin, J. Grilj, Y. P. Tsentalovitch and E. Vauthey, Ultrafast Excited-State Dynamics of Kynurenine, a UV Filter of the Human Eye, *J. Phys. Chem. B*, 2009, **113**, 4953–4962.
36 J.-P. Malval, V. Diemer, F. Morlet-Savary, P. Jacques, H. Chaumeil, A. Defoin, C. Carré and O. Poizat, Photoinduced Coupled Charge and Proton Transfers in Gradually Twisted Phenol-Pyridinium Biaryl Series, *J. Phys. Chem. A*, 2010, **114**, 2401–2411.
37 S. J. Rosenthal, X. Xie, M. Du and G. R. Fleming, Femtosecond solvation dynamics in acetonitrile: observation of the inertial contribution to the solvent response., *J. Chem. Phys.*, 1991, **95**, 4715.
38 R. M. Stratt and M. Maroncelli, Nonreactive Dynamics in Solution: The Emerging Molecular View of Solvation Dynamics and Vibrational Relaxation, *J. Phys. Chem.*, 1996, **100**, 12981–12996.
39 J. Jortner and M. Bixon, Intramolecular vibrational excitations accompanying solvent controlled electron transfer reactions., *J. Chem. Phys.*, 1988, **88**, 167.
40 N. R. Kestner, J. Logan and J. Jortner, Thermal electron transfer reactions in polar solvents, *J. Phys. Chem.*, 1974, **78**, 2148–2166.
41 R. A. Marcus and N. Sutin, Electron transfer in chemistry and biology., *Biochim. Biophys. Acta, Rev. Bioenerg.*, 1985, **811**, 265–322.
42 I. R. Gould, D. Noukakis, J. L. Goodman, R. H. Young and S. Farid, A quantitative relationship between radiative and non radiative electron transfer in radical ion pairs., *J. Am. Chem. Soc.*, 1993, **115**, 3830.
43 E. Vauthey, Effect of steric hindrance on the dynamics of charge recombination within geminate ion pairs, *J. Phys. Chem. A*, 2000, **104**, 1804.
44 P. Jacques, D. Burget and X. Allonas, On the quantitative appraisal of the free energy change in photoinduced electron transfer, *New J. Chem.*, 1996, **20**, 933.
45 H. Sumi, Theory on rates of solution reactions influenced by slow fluctuations in viscous solvents, and its experimental confirmation, *J. Mol. Liq.*, 1995, **65–66**, 65.
46 H. Sumi and R. A. Marcus, Dynamical effects in electron transfer reactions., *J. Chem. Phys.*, 1986, **84**, 4894.
47 A. Pigliucci, G. Duvanel, M. L. Lawson Daku and E. Vauthey, Investigation of the Influence of Solute–solvent Interactions on the Vibrational Energy Relaxation Dynamics of Large Molecules in Liquids, *J. Phys. Chem. A*, 2007, **111**, 6135–6145.
48 C. T. Middleton, B. Cohen and B. Kohler, Solvent and Solvent Isotope Effects on the Vibrational Cooling Dynamics of a DNA Base Derivative, *J. Phys. Chem. A*, 2007, **111**, 10460–10467.
49 J. C. Owrutsky, D. Raftery and R. M. Hochstrasser, Vibrational-Relaxation Dynamics in Solutions, *Annu. Rev. Phys. Chem.*, 1994, **45**, 519–555.
50 P. K. McCarthy and G. J. Blanchard, Solvent methyl group density dependence of vibrational population relaxation in 1-methylperylene: evidene for short range organisation in branched alkanes, *J. Phys. Chem.*, 1996, **100**, 5182.
51 J. Assmann, A. Charvat, D. Schwarzer, C. Kappel, K. Luther and B. Abel, Real-Time Observation of Intra- and Intermolecular Vibrational Energy Flow of Selectively Excited Alkyl Iodides in Solution: The Effect of Chemical Substitution, *J. Phys. Chem. A*, 2002, **106**, 5197.
52 K. Iwata and H. Hamaguchi, Vibrational cooling process in solution probed by picosecond time-resolved Raman spectroscopy. Analysis of the cooling kinetics., *J. Mol. Liq.*, 1995, **65–66**, 417.
53 A. C. Benniston, P. Matousek, I. E. McCulloch, A. W. Parker and M. Towrie, Detailed Picosecond Kerr-Gated Time-Resolved Resonance Raman Spectroscopy and Time-Resolved Emission Studies of Merocyanine 540 in Various Solvents, *J. Phys. Chem. A*, 2003, **107**, 4347.
54 C. V. Bindhu, S. S. Harilal, V. P. N. Nampoori and C. P. G. Vallabhan, Thermal diffusivity measurements in organic liquids using transient thermal lens calorimetry, *Opt. Eng.*, 1998, **37**, 2791–2794.